Title
Is Subsurface Oxygen Necessary for the Electrochemical Reduction of CO2 on Copper?

Journal
The journal of physical chemistry letters, 9(3)

ISSN
1948-7185

Authors
Garza, Alejandro J
Bell, Alexis T
Head-Gordon, Martin

Publication Date
2018-02-01

DOI
10.1021/acs.jpclett.7b03180

Peer reviewed

Is Subsurface Oxygen Necessary for the Electrochemical Reduction of CO_2 on Copper?

Alejandro J. Garza,[1] Alexis T. Bell,[2] and Martin Head-Gordon[3]

[1]Joint Center for Artificial Photosynthesis, Lawrence Berkeley National Laboratory, Berkeley, California 94720, USA, [2]Department of Chemical and Biomolecular Engineering, University of California at Berkeley, Berkeley, California 94720, United States, and [3]Department of Chemistry, University of California at Berkeley, Berkeley, California 94720, United States

AUTHOR INFORMATION

alexbell@berkeley.edu; mhg@cchem.berkeley.edu

ABSTRACT. It has recently been proposed that subsurface oxygen is crucial for the adsorption and subsequent electroreduction of CO_2 on copper. Using density functional theory, we have studied the stability and diffusion of subsurface oxygen in single crystals of copper exposing (111) and (100) facets. Oxygen is at least 1.5 eV more stable on the surface than beneath it for both crystal orientations; interstitial sites are too small to accommodate oxygen. The rate of atomic oxygen diffusion from one layer below a Cu(111) surface to the surface is 5×10^3 s^{-1}. Oxygen can survive longer in deeper layers, but it does not promote CO_2 adsorption there. Diffusion of subsurface oxygen is easier to the less-dense Cu(100) surface, even from lower layers (rate $\approx 1\times10^7$ s^{-1}). Once the applied voltage and dispersion forces are properly modeled, we find that subsurface oxygen is unnecessary for CO_2 adsorption on copper.

TOC GRAPHICS

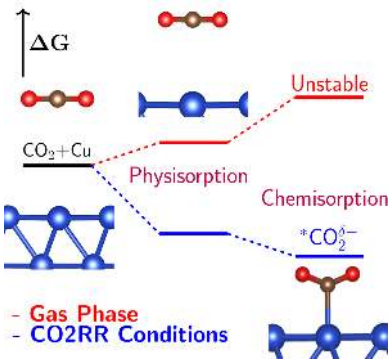

KEYWORDS. Artificial Photosynthesis, Catalysis, Modeling, Semilocal DFT, Nonlocal DFT

Copper is the only monometallic catalyst that promotes the electrochemical reduction of CO_2 to hydrocarbons and alcohols with high faradaic efficiency.[1,2] A number of authors have reported that the activity of copper and its selectivity to form C_2 products (ethene and ethanol) are enhanced when copper is first oxidized and then reduced.[3-10] This observation has led to the suggestion that oxide-derived copper either retains an oxide phase or subsurface oxygen under the conditions used for the CO_2 reduction reaction (CO2RR) (i.e., at cathode potentials below –0.9 V vs RHE).[11-21] While *in situ* X-ray absorption near edge spectroscopy (XANES), *in situ* atmospheric pressure X-ray absorption spectroscopy (APXPS), and *quasi in situ* electron energy loss spectroscopy (EELS) have shown that Cu_2O formed under oxidizing conditions is reduced to metallic Cu at a cathode potentials below 0.35 V vs RHE,[16,21] experimental evidence has been reported for the retention of subsurface oxygen based upon *quasi in situ* X-ray photoelectron spectroscopy (XPS), EELS conducted in a scanning transmission electron microscope (STEM), imaging by TEM and STEM, and positron annihilation spectroscopy (PAS).[14-17] Theoretical studies have also concluded that subsurface oxygen enables the adsorption of CO_2 and promotes the coupling of adsorbed CO to form C-C bonds, suggesting that the enhanced activity and

selectivity formation of C_2 products observed during the CO2RR on oxide-derived Cu is attributable to subsurface oxygen.[14,20]

A critical question regarding the effects of subsurface oxygen on the activity and selectivity of oxide-derived Cu for the CO2RR is whether or not this species is stable under the highly reducing conditions used for this reaction. This question has recently been addressed by experiments using ^{18}O-labeled water.[22] An electrochemically roughened Cu foil was first oxidized under anodic conditions in an $H_2{}^{18}O$ solution of $KHCO_3$ and KCl to form a ~100 nm thick layer of Cu_2O. *Ex situ* secondary ion mass spectrometry (SIMS) showed the content of ^{18}O near the sample surface to be ~10^{22} atoms/cm^3, consistent with that expected for a bulk copper oxide phase. The oxidized sample was then used to catalyze the CO2RR in aqueous 0.1 M $KHCO_3$. *Ex situ* SIMS measurements made after 30 min, 1 h, and 5 h of reaction revealed that even after 30 min of reaction at a cathode voltage of –1 V vs RHE, the ^{18}O content of the catalyst decreased to less than 1% of that measured before reaction, and was very close to the natural abundance of ^{18}O in water. Subsequent experiments demonstrated that the oxygen content of Cu is rapidly restored by rinsing freshly-reduced oxide-derived Cu produced under conditions of the CO2RR in deionized water for 3 min. The results of this work suggest that the concentration of subsurface oxygen present in Cu under the highly reducing conditions used for the CO2RR is very small (< 1%) and that the reoxidation of reduced copper by H_2O (possibly due to dissolved O_2) is very rapid. The findings of this study place into question whether the subsurface oxygen reported in previous experimental studies is oxygen that has been retained from the peroxidation of Cu or, rather, introduced during the removal of the reduced sample from the electrolyte and the subsequent preparation of the sample for analysis.[22]

The present study was undertaken to determine the stability of subsurface oxygen under the conditions used for the CO2RR and to establish whether surface oxygen is essential for the adsorption of CO_2. We report here DFT-based simulations demonstrating that subsurface oxygen would not survive for long near the surface of Cu under conditions typically used for the CO2RR. We also find that physisorption of CO_2 on copper becomes thermodynamically favorable once solvent and nonlocal correlation effects are taken into account. Similarly, chemisorption to form bent, negatively-charged CO_2 (b-CO_2) on the surface is not favorable unless the effect of the applied voltage is taken into account. This is achieved by adjusting the number of electrons in the unit cell so that the Fermi level of the metal matches the applied potential; excess surface charge is neutralized by the electrolyte charge from the linearized Poisson-Boltzmann equation. Further details concerning this methodology and the calculation of free energies may be found elsewhere.[23-25]

Figure 1 shows the free energy profile at 298 K for the migration of an oxygen atom from a tetrahedral site right below the surface (T_-^I) to a hole site on the Cu(111) surface at various potentials. These calculations were carried out using the Perdew-Burke-Ernhzerhof (PBE) functional in VASP[26] (plane-wave energy cutoff = 500 eV, 4×4×1 k-mesh); the electrolyte is represented by the linearized Poisson-Boltzmann model implemented in VASPsol[27,28] ([KCO_3H] = 0.1 M). Four layers of Cu atoms were used to model the slab. A tetrahedral site with an oxygen coverage of θ = ¼ was chosen as these specific parameters were found to be critical for enabling CO_2 adsorption.[14] Figure 1 suggests that this subsurface oxygen configuration is unstable: the process of moving from the T_-^I site to the surface has a Gibbs free energy of activation ($\Delta G^{\ddagger}$) of 0.33 eV and a Gibbs free energy of reaction (ΔG) of −1.51 eV in the absence of an applied bias. Calculations at −0.5 and −1.0 V vs. the RHE (pH = 7) show that the potential dependence for this

process is relatively weak: $\Delta G^{\ddagger}$ = 0.35 eV and $\Delta G \approx -1.75$ eV at both of these voltages. Distortions of the lattice in the subsurface oxide structure reveal that the T_-^I site is too small to properly accommodate an oxygen atom, accounting for the thermodynamic instability of this structure. Electronic repulsion between Cu and O atoms increases when the surface is negatively charged, resulting in further destabilization of subsurface oxygen in the presence of an applied voltage. The low kinetic barrier is a consequence of the relative freedom of movement for atoms on the topmost layer. For $\Delta G^{\ddagger}$ = 0.35 eV, the absolute rate theory gives a turnover frequency (TOF) of 7.6×10^{6} s^{-1} per O atom.

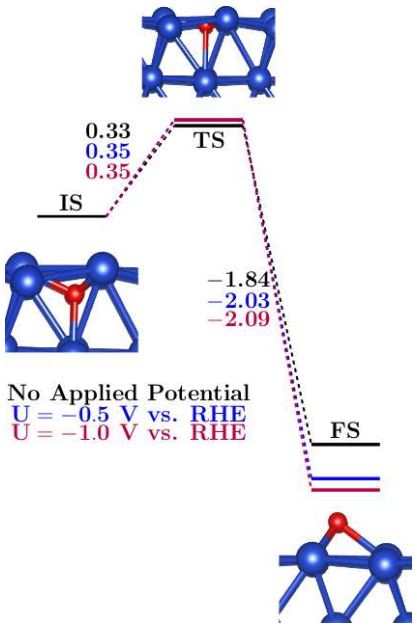

Figure 1. Free energy profile (in eV) for migration of an oxygen atom occupying a tetrahedral site below the surface to a hole site on the surface at various potentials (θ = ¼, pH = 7).

The results of figure 1, however, do not rule out the possibility that oxygen is stable in a different subsurface locale. Three types of site are available on a close-packed (111) lattice: octahedral (O_h) sites, tetrahedral sites that allow for upward interstitial diffusion (T_-), and

tetrahedral sites that do not allow for upward diffusion (T_+). On a (100) facet, only two types of site, octahedral (o_h) and tetrahedral (t_d), are accessible. An atom on an o_h site can diffuse to a t_d site on the same level and subsequently migrate to an upper o_h location. Figure 2 maps the pathways by which migration between these sites and to the surface may occur; the notation is the same as the one we have just defined with an added Roman numeral superscript indicating the layer depth with respect to the surface. The first two layers below the surface are considered (oxygen deeper in the lattice is not expected to have much of an effect on the ability of the surface to bind CO_2).

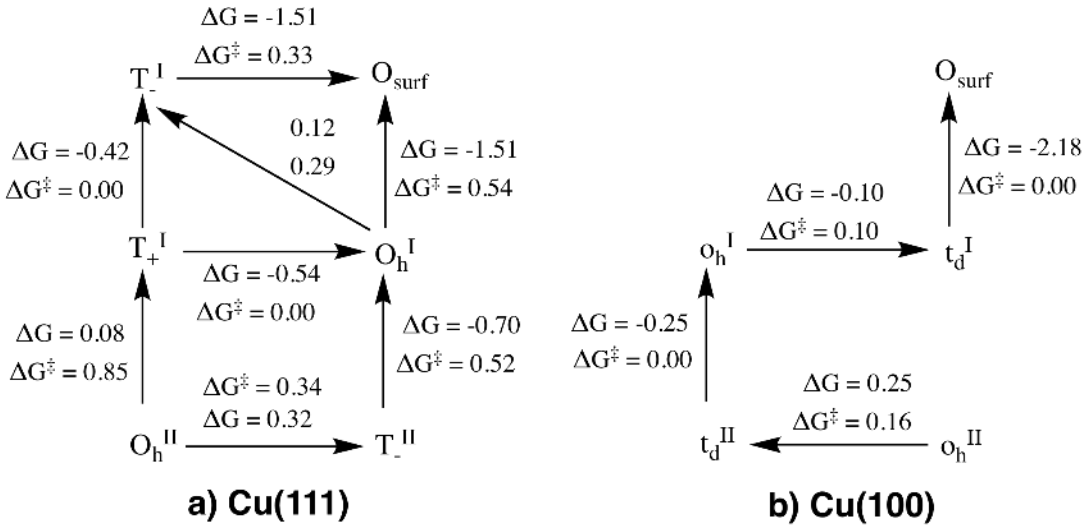

Figure 2. Oxygen diffusion pathways from the second layer (II) below the surface to the first subsurface layer (I) and the surface of (a) Cu(111) and (b) Cu(100). O_{surf} denotes any available surface site; the rest of the notation is defined in the text. Energies are in eV.

Figure 2 shows octahedral sites to be generally more stable than tetrahedral sites by about 0.3 eV. This observation is consistent with the idea that an overly small cavity size is responsible for the instability of subsurface oxygen; based solely on trigonometry, octahedral sites are 1.84 times larger than tetrahedral ones. Exceptions arise for the T_-^I and t_d^I sites, which can be rationalized by the fact that these locations are open to the surface, and hence experience less

confinement. We utilized the energetic span model[29-31] to determine the TOFs for oxygen atoms on the O_h^{II} and o_h^{II} sites to reach the surface. Based on the data from figure 2, this model yields a TOF = 3×10^{-2} s^{-1} for the O_h^{II} site of Cu(111) and a TOF > 7.6×10^{6} s^{-1} for the o_h^{II} site in Cu(100). The more open, less-coordinated (100) facet is therefore unable to retain oxygen under the two topmost copper layers for any significant amount of time. On the more dense Cu(111), the lifetime of oxygen under the second layer is on the scale of a few minutes. Note that the TOF of diffusion from the second layer of 3×10^{-2} s^{-1} calculated for Cu(111) corresponds to an effective $\Delta G^{\ddagger}$ of about 0.84 eV, and that the experimental $\Delta G^{\ddagger}$ for bulk copper is 0.69 eV.[32] Our computed free energy barriers may be overestimated because of the use of periodic boundary conditions, which cause structural disruptions in the surface to repeat throughout the crystal. Barriers computed at lower O coverages are thus expected to be smaller. Despite the possible overestimation of $\Delta G^{\ddagger}$ values, the calculations predict that copper is unable to kinetically trap near-surface oxygen for time spans relevant to the CO2RR. Although we have only considered Cu(111) and Cu(100) surfaces, the results suggest that any surface that is less densely packed than Cu(111) would be even less likely to retain oxygen due to the greater mobility of undercoordinated surface atoms.

A low kinetic and thermodynamic stability of near-surface oxygen implies that subsurface oxygen is not required for CO_2 reduction on metallic copper. However, this is at odds with previous DFT calculations, which conclude that CO_2 does not adsorb on a pure Cu(111) surface.[14] Reconciliation of this contradiction requires careful examination of how the entropy of adsorption is determined and the impact of the density functional used in the simulations. Favaro et al.[14] report a physisorption enthalpy, ΔH_{phys}, of –0.30 eV, but a positive free energy of physisoption (ΔG_{phys} = 0.27 eV) based on calculations made using a semilocal functional

(M06L). These calculations do not include solvent effects and employ ideal gas formulas to compute thermal entropic contributions to ΔG. However, it is known that rigid rotor and harmonic oscillator formulas overestimate the entropy of molecules in solution because the translational and rotational motions of the solute are reduced by the surrounding solvent molecules.[23,34] From Henry's law data, the entropy of $CO_{2(g)}$ is 126.0 J/mol·K larger than that of $CO_{2(aq)}$,[35,36] which corresponds to an increase of 0.39 eV in the $-T\Delta S$ term of the free energy of $CO_{2(aq)}$ relative to $CO_{2(g)}$ at 298 K. This suggests that CO_2 may physisorb on copper when dissolved in water, as it is during the CO2RR. We will elaborate on this point and report the results from our own calculations below.

A second factor that can explain the adsorption of CO_2 on copper is related to the limitations of semilocal correlation functionals, which to the best of our knowledge are utilized in all previous relevant theoretical studies. The correlation in functionals such as PBE or M06 depends only on semilocal quantities (i.e., the density and density gradients). As a consequence, attraction vanishes exponentially with the distance between molecules or a molecule and a surface.[37] In other words, semilocal approximations cannot describe—not even in principle—long-range dispersion correlation (e.g., van der Waals forces). For these reasons we have used the SCAN+rVV10 functional,[38] which incorporates nonlocal correlation, to estimate the physisorption of CO_2 with copper. SCAN+rVV10 was designed with applications to the solid-state in mind and has minimal empiricism; it satisfies all known exact constraints a functional of its kind can satisfy,[39] thus avoiding training set bias (which may favor accuracy for molecular systems over extended ones). Moreover, we take into account the aforementioned reduction of the entropy of CO_2 in water, as well as the effects of the applied potential, as detailed above. The

applied voltage is, in fact, a third factor that may explain CO_2 adsorption during the CO2RR, and as we will see shortly, it is indeed critical for CO_2 chemisorption.

Table 1 summarizes the SCAN+rVV10 results for the adsorption of CO_2 on copper under various conditions. These data indicate that CO_2 adsorbs on Cu under CO2RR conditions at moderate pressures. Physisorption of $CO_{2(aq)}$ is predicted to be exergonic on both Cu(111) and Cu(100) under all conditions considered. Depending on the surface, voltage, and coverage, ΔG_{phys} varies from –0.10 eV to –0.30 eV. Based on the results of our geometry optimizations, the structure of the chemisorbed *b*-CO_2 species appears to be unstable in the absence of an applied potential. However, with a voltage of $U = -1$ V vs RHE chemisorption is also exergonic; this suggests that a negatively charged surface is needed to stabilize *b*-CO_2. On Cu(111), physisorption is favored over chemisorption at a coverage of $\theta = ¼$. Nevertheless, at a more realistic $\theta = ⅛$, *b*-CO_2 is preferred. Recall that *b*-CO_2 has a partial negative charge that would generate electrostatic repulsion between neighboring adsorbates; thus the need for a lower coverage to favor *b*-CO_2 formation. On Cu(100), chemisorption is favored even at the high $\theta = ¼$. The Cu atoms on a (100) surface are less coordinated and hence more reactive and able to chemically bind CO_2. Notice that *b*-CO_2 is the first reactive species in the CO2RR mechanism, and that Cu(100) is more active toward CO_2 reduction than Cu(111).[40] Another interesting observation is that while the applied potential has a stabilizing effect on *b*-CO_2, it slightly suppresses physisorption. Presumably, the reason for favoring chemisorption under an applied voltage is that *b*-CO_2 acts essentially as a Lewis acid, whereas a possible reason for disfavoring physisorption is steric or electrostatic repulsion between CO_2 and the charged surface.

Table 1. Free energies for physisorption and chemisorption of $CO_{2(aq)}$ on Cu(111) and Cu(100) under various conditions calculated with the SCAN+rVV10 functional in an electrolyte medium.

Surface	*Coverage*	*Voltage/V*	$\Delta G_{phys}/eV$	$\Delta G_{chem}/eV$
Cu(111)	¼	0.0	–0.30	NA[†]
Cu(111)	¼	–1.0 vs RHE	–0.21	–0.12
Cu(111)	⅛	–1.0 vs RHE	–0.10	–0.21
Cu(100)	¼	0.0	–0.35	NA[†]
Cu(100)	¼	–1.0 vs RHE	–0.29	–0.39

[†]Ion relaxation did not yield a chemisorbed geometry for CO_2.

We assessed the possibility of oxygen beneath the second layer of Cu(111) affecting CO_2 adsorption (the estimated lifetimes of oxygen on Cu(100) and the first layer of Cu(111) are too low to be worth considering). Contrary to the reported large, cooperative effect of oxygen on T_-^I sites,[1] oxygen under the second layer has a modest, detrimental influence on CO_2 physisorption: the ΔG_{phys} = –0.30 eV on pure Cu(111) with θ = ¼ increases to –0.15 eV on the suboxide surface. The weakening of physisorption appears to be rooted in the high electronegativity of oxygen: an inductive effect contracts the Cu orbitals that can interact with CO_2 in the long range. The effect is subtle, but it can be appreciated in the projected density of states for 4*s* orbitals in figure 3. The energetic range of 4*s* states in the pure Cu(111) and the corresponding suboxide structure indicate that 4*s* orbitals in the latter are more localized. These orbitals are the most diffuse occupied orbitals in Cu, and would therefore contribute significantly to the overlap with CO_2 density when far apart from the surface.

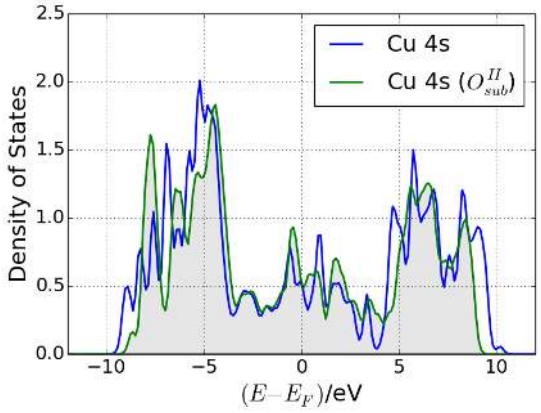

Figure 3. Projected density of states computed with the SCAN+rVV10 functional for 4*s* orbitals of pure Cu(111) and Cu(111) with oxygen beneath the second topmost layer (θ =1/4).

For chemisorption, the effect of subsurface oxygen below the second layer of Cu(111) is negligible: at –1.0 vs RHE and θ =1/4, SCAN+rVV10 gives ΔG_{chem} = –0.14 and –0.12 eV value for the suboxide and pure Cu(111) surfaces, respectively.

It is worth mentioning that our calculated adsorption free energies do not consider the effect of pressure and concentration on the chemical potentials (see ref. 23 for the free energy formulas used here). Under typical reaction conditions, these effects do not affect our qualitative findings. For example, the chemisorption free energies for $CO_{2(g)}$ at 298 K and 1 atm on Cu(111) and Cu(100) would be 0.08 (θ =1/8) and –0.1 eV (θ =1/4), respectively. The values are higher than those in Table 1 due to the increased entropy of $CO_{2(g)}$ as compared to $CO_{2(aq)}$, but still predict CO_2 to chemisorb to a degree that makes it possible for the reaction to take place: adsorption is thermodynamically favorable on Cu(100) and, assuming ΔG_{chem} does not increase with lower coverage, the Langmuir isotherm curve for Cu(111) predicts a coverage of about 1/20 at 298 K and 1 atm.

In summary, our results suggest that subsurface oxygen does not play a key role during the CO2RR on Cu. Near-surface oxygen is not sufficiently long-lived to be present during the reaction; moreover, theory predicts that copper can adsorb CO_2 without the need for subsurface oxygen (once dispersion interactions, electrolyte, and voltage are taken into account in the modeling). We suggest that, rather than subsurface oxygen, surface defects introduced during the electrochemical reduction of oxidized copper may be responsible for the observed enhancements in the CO2RR activity and selectivity to ethylene and ethanol reported for oxide-derived copper. As noted earlier, oxygen is too large to fit into the interstitial sites of copper. Thus, for interstitial diffusion to occur oxygen must significantly disrupt the positions of adjacent Cu atoms in the lattice; this is indeed reflected in our transition state structures (see figure 4). This process may leave behind defects such as holes and under-coordinated surface atoms that promote CO_2 adsorption and CO dimerization—the fact that less-coordinated atoms favor these processes is clear when comparing energetics on the Cu(111) and Cu(100) surfaces reported here and elsewhere.[25,41,42] Recent investigations of the CO2RR on Cu and Ag also support the hypothesis that surface defects are responsible for the properties of oxide-derived copper catalysts.[17,43]

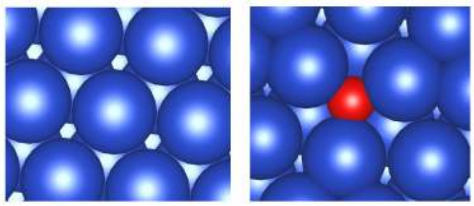

Figure 4. A clean Cu(111) surface (left) and the transition state for O diffusion from a O_h^I site to the surface.

The present study also demonstrates that the oxidation of Cu(111) by O_2 to form surface and subsurface oxygen is strongly favored thermodynamically. The free energies of sorption per oxygen atom ΔG_{sorp} estimated with the SCAN+rVV10 functional are –5.93, –4.55, and –4.03 eV

for the surface, O_h^I, and O_h^{II} sites, respectively, in reasonable agreement the experimentally measured value of –4.47 eV.[44] Thus, even at extremely low O_2 partial pressures ($\approx 1\times10^{-72}$ Torr at 298 K), oxygen capture at surface and subsurface sites is thermodynamically favored. The very high sensitivity of reduced Cu to oxidation is also confirmed by the observation of subsurface oxygen in ultrahigh vacuum studies at pressures as low as 5×10^{-8} Torr.[45] Hence, we suggest that it is virtually impossible to preclude the oxidation of fully reduced Cu by trace amounts of oxygen present in water once Cu is no longer under a reducing potential. We also note that O_2 sorption and the instability of subsurface oxygen relative surface oxygen that we report here are in agreement with previous theoretical studies of surface oxides on Cu(111)[46,47] and with the recently reported work carried out using ^{18}O labeled water discussed earlier in the text.[22]

Given the findings here, it is worth considering alternatives that could stabilize subsurface oxygen. One possibility is that O-induced surface reconstruction contributes to stabilization of subsurface oxygen. While O-induced reconstruction has been observed on Cu(100),[48] this possibility is unlikely to stabilize subsurface oxygen for three reasons: (1) surface reconstruction results in a high concentration undercoordinated surface atoms,[48] which as was mentioned above are expected to facilitate O diffusion and (2) EC-LEED-AES[49] and *operando* ECSTM[50.51] measurements indicate that pre-oxidized copper surfaces revert to well-ordered metallic structures the during the electrochemical reduction of CO_2. A closely related explanation for the stability of subsurface oxygen in Cu nanoparticles has been proposed recently by Nilsson and co-workers.[17,18] The authors suggest that subsurface oxygen is stabilized by the formation of an amorphous layer (~2nm thick) of copper on the surface Cu nanoparticles (diameter 20-100 nm). This conclusion is drawn from *quasi in situ* HRTEM and STEM-ADF observations of Cu

nanoparticles following their use for the CO2RR. This hypothesis is supported by theoretical calculations.[18] Using self-consistent charge density functional tight binding methods, the authors conclude that model oxide-derived copper nanocubes (of 500 Cu atoms) become amporphous as oxygen atoms are removed from their surface and that subsurface oxygen is more stable in the resulting amorphous material. It is notable that the authors of this work find, as do we, that subsurface O is not stable on a Cu(100) film.[18]

While the role of amorphous Cu in stabilizing subsurface oxygen is plausible, the question still remains as to whether the subsurface oxygen observed experimentally was not introduced unintentionally during the removal of the sample from the electrolyte in dry nitrogen and subsequent rinsing of the residual electrolyte from the sample using de-aerated water. This possibility is strongly suggested by the ^{18}O labeling experiments of Ager and Lum[22] and by our calculations, both of which show the strong susceptibility of reduced Cu to even very trace amounts of O_2.

It is appropriate to conclude with a brief mention of the remaining limitations of our calculations. We have improved the density functional approximation relative to previous studies by incorporating nonlocal correlation, but it is still an approximation and there may be remaining errors. We have accounted for finite bias in the electronic structure and for the effect of the electrolyte using continuum descriptions, but it is likely that the continuum approximation is not fully adequate. However, this issue is unlikely to affect our results as specific solvent-CO_2 and ion-CO_2 interactions are probably not at play (and if so would tend to further stabilize *b*-CO_2). Furthermore, our findings are in agreement experimental observations[22,45] and with other theoretical studies that employ methodologies different from the one used here.[18,46,47] We believe that our results align theory and experiment regarding the role of subsurface oxygen on the

CO2RR in light of the ^{18}O experiments of Lum and Ager[22] demonstrating that oxide-derived Cu catalysts do not retain even traces of the original oxygen during reaction.

ACKNOWLEDGMENT

This material is based on work performed in the Joint Center for Artificial Photosynthesis, a DOE Energy Innovation Hub, supported through the Office of Science of the U.S. Department of Energy under Award DE-SC00004993. This research used resources of the National Energy Research Scientific Computing Center, a DOE Office of Science User Facility supported by the Office of Science of the U.S. Department of Energy under Contract No. DE-AC02-05CH11231.

REFERENCES

(1) Hori, Y. Electrochemical CO_2 Reduction on Metal Electrodes. In *Modern Aspects of Electrochemistry*; Springer, 2008; pp 89-189.

(2) Kuhl, K. P.; Cave, E. R.; Abram, D. N.; Jaramillo, T. F. New Insights into the Electrochemical Reduction of Carbon Dioxide on Metallic Copper Surfaces. *Energy Environ. Sci.* **2012**, 5, 7050.

(3) Li, C. W.; Ciston, J.; Kanan, M. W. Electroreduction of carbon monoxide to liquid fuel on oxide-derived nanocrystalline copper. *Nature* **2014**, 508, 504-507.

(4) Kas, R.; Kortlever, R.; Milbrat, A.; Koper, M. T. M.; Mul, G.; Baltrusaitis, J. Electrochemical CO_2 Reduction on Cu_2O-Derived Copper Nanoparticles: Controlling the Catalytic Selectivity of Hydrocarbons. *Phys. Chem. Chem. Phys.* **2014**, 16, 12194.

(5) Ren, D.; Deng, Y.; Handoko, A. D.; Chen, C. S.; Malkhandi, S.; Yeo, B. S. Selective Electrochemical Reduction of Carbon Dioxide to Ethylene and Ethanol on Copper(I) Oxide Catalysts. *ACS Catal*. **2015**, 5, 2814-2821.

(6) Roberts, F. S.; Kuhl, K. P.; Nilsson, A. High Selectivity for Ethylene from Carbon Dioxide Reduction over Copper Nanocube Electrocatalysts. *Angew. Chem*. **2015**, 127, 5268-5271.

(7) Ma, M.; Djanashvili, K.; Smith, W. A. Selective Electrochemical Reduction of CO_2 to CO on CuO-Derived Cu Nanowires. *Phys. Chem. Chem. Phys*. **2015**, 17, 20861-20867.

(8) Dutta, A.; Rahaman, M.; Luedi, N. C.; Mohos, M.; Broekmann, P. Morphology Matters: Tuning the Product Distribution of CO2 Electroreduction on Oxide-Derived Cu Foam Catalysts. *ACS Catal*. **2016**, 6, 3804-3814.

(9) Lum, Y.; Yue, B.; Lobaccaro, P.; Bell, A.T.; Ager, J.W., 2017. Optimizing CC Coupling on Oxide-Derived Copper Catalysts for Electrochemical CO_2 Reduction. *J. Phys. Chem. C* **2017**, 121, 1491-14203.

(10) Zhao, K.; Liu, Y.; Quan, X.; Chen, S.; Yu, H. CO_2 Electroreduction at Low Overpotential on Oxide-Derived Cu/Carbons Fabricated from Metal Organic Framework. *ACS Appl. Mater. Interfaces* **2017**, 9, 5302-5311.

(11) Kim, D.; Lee, S.; Ocon, J. D.; Jeong, B.; Lee, J. K.; Lee, J. K.; Wang, H. L.; Norskøv, J. K.; Chorkendorff, I.; Lee, K.; et al. Insights into Autonomously Formed Oxygen-Evacuated Cu_2O Electrode for the Selective Production of C_2H_4 from CO_2. *Phys. Chem. Chem. Phys*. **2014**, 17, 1-9.

(12) Lee, S.; Kim, D.; Lee, J. Electrocatalytic Production of C3-C4 Compounds by Conversion of CO_2 on a Chloride-Induced Bi-Phasic Cu_2O-Cu Catalyst. *Angew. Chem*. **2015**, 127, 14914-14918.

(13) Mistry, H.; Varela, A. S.; Bonifacio, C. S.; Zegkinoglou, I.; Sinev, I.; Choi, Y.-W.; Kisslinger, K.; Stach, E. A.; Yang, J. C.; Strasser, P.; et al. Highly Selective Plasma-

Activated Copper Catalysts for Carbon Dioxide Reduction to Ethylene. *Nat. Commun.* **2016**, 7, 12123.

(14) Favaro, M.; Xiao, H.; Cheng, T., Goddard, W.A.; Yano, J.; Crumlin, E.J. Subsurface oxide plays a critical role in CO_2 activation by Cu (111) surfaces to form chemisorbed CO_2, the first step in reduction of CO_2. *Proc. Natl. Acad. of Sci.* **2017**, 114, 6706-6711.

(15) Gao, D.; Zegkinoglou, I.; Divins, N.J.; Scholten, F.; Sinev, I.; Grosse, P.; Roldan Cuenya, B. Plasma-Activated Copper Nanocube Catalysts for Efficient Carbon Dioxide Electroreduction to Hydrocarbons and Alcohols. *ACS Nano* **2017**, 11, 4825-4831.

(16) Eilert, A.; Cavalca, F.; Roberts, F.S.; Osterwalder, J.; Liu, C.; Favaro, M.; Crumlin, E.J.; Ogasawara, H.; Friebel, D.; Pettersson, L.G.; Nilsson, A. Subsurface Oxygen in Oxide-Derived Copper Electrocatalysts for Carbon Dioxide Reduction. *J. Phys. Chem. Lett.* **2016**, 8, 285-290.

(17) Cavalca, F.; Ferragut, R.; Aghion, S.; Eilert, A.; Diaz-Morales, O.; Liu, C.; Koh, A.L.; Hansen, T.W.; Pettersson, L.G.; Nilsson, A. Nature and Distribution of Stable Subsurface Oxygen in Copper Electrodes During Electrochemical CO_2 Reduction. *J. Phys. Chem. C* **2017**. DOI: 10.1021/acs.jpcc.7b08278.

(18) Liu, C.; Lourenço, M.P.; Hedström, S.; Cavalca, F.; Diaz-Morales, O.; Duarte, H.A.; Nilsson, A.; Pettersson, L.G. Stability and Effects of Subsurface Oxygen in Oxide-Derived Cu Catalyst for CO_2 Reduction. *J. Phys. Chem. C* **2017**. DOI: 10.1021/acs.jpcc.7b08269.

(19) Engelbrecht, A.; Hämmerle, M.; Moos, R.; Fleischer, M.; Schmid, G. Improvement of the selectivity of the electrochemical conversion of CO_2 to hydrocarbons using cupreous electrodes with in-situ oxidation by oxygen. *Electrochimica Acta* **2017**, 224, 642-648.

(20) Xiao, H.; Goddard, W.A.; Cheng, T.; Liu, Y. Cu metal embedded in oxidized matrix catalyst to promote CO_2 activation and CO dimerization for electrochemical reduction of CO_2. *Proc. Natl. Acad. of Sci.* **2017**, 114, 6685-6688.

(21) Eilert, A.; Roberts, F. S.; Friebel, D.; Nilsson, A. Formation of Copper Catalysts for CO_2 Reduction with High Ethylene/Methane Product Ratio Investigated with In Situ X-Ray Absorption Spectroscopy. J. Phys. Chem. Lett. **2016**, 7, 1466–1470.

(22) Lum, Y.; Ager, J. W. Stability of residual oxides in oxide-derived Cu catalysts for electrochemical CO_2 reduction investigated with ^{18}O labeling. *Angew. Chem. Int. Ed.* **2017**. DOI: 10.1002/anie.201710590.

(23) Jinnouchi, R.; Anderson, A. B. Electronic structure calculations of liquid-solid interfaces: Combination of density functional theory and modified Poisson-Boltzmann theory. *Phys. Rev. B* **2008**, 77, 245417.

(24) Goodpaster, J. D.; Bell, A. T.; Head-Gordon, M. Identification of Possible Pathways for C-C Bond Formation during Electrochemical Reduction of CO_2: New Theoretical Insights from an Improved Electrochemical Model. *J. Phys. Chem. Lett.* **2016**, 7, 1471-1477.

(25) Garza, A. J.; Bell, A. T.; Head-Gordon, M. On the Mechanism of CO_2 Reduction at Copper Surfaces: Pathways to C_2 Products. *ACS Catal.* 2018, DOI: 10.1021/acscatal.7b03477.

(26) Kresse, G.; Furthmüller, J. Efficient iterative schemes for ab initio total-energy calculations using a plane-wave basis set. *Phys. Rev. B* **1996**, 54, 11169.

(27) Mathew, K. Henning, R. G. Implicit self-consistent description of electrolyte in plane-wave density-functional theory. **2016**, arXiv:1601.03346 [cond-mat.mtrl-sci].

(28) Mathew, K.; Sundararaman, R. Letchworth-Weaver, K.; Arias, T. A.; Hennig, R. G. Implicit solvation model for density-functional study of nanocrystal surfaces and reaction pathways. *J. Chem. Phys.* **2014**, 140, 084106.

(29) Kozuch, S.; Shaik, S. A combined kinetic-quantum mechanical model for assessment of catalytic cycles: application to cross-coupling and Heck reactions. *J. Am. Chem. Soc.* **2006**, 128, 3355-3365.

(30) Kozuch, S.; Shaik, S. Kinetic-Quantum Chemical Model for Catalytic Cycles: The Haber-Bosch Process and the Effect of Reagent Concentration. *J. Phys. Chem. A* **2008**, 112, 6032-6041.

(31) Kozuch, S.; Martin, J.M. What makes for a bad catalytic cycle? A theoretical study on the Suzuki-Miyaura reaction within the energetic span model. *ACS Catal.* **2011**, 1, 246-253.

(32) Narula, M.L.; Tare, V.B.; Worrell, W.L. Diffusivity and solubility of oxygen in solid copper using potentiostatic and potentiometric techniques. *Metallurgical Transactions B* **1983**, 14, 673-677.

(33) Sumimoto, M.; Iwane, N.; Takahama, T.; Sakaki, S. Theoretical study of trans-metalation process in palladium-catalyzed borylation of iodobenzene with diboron. *J. Am. Chem. Soc.* **2004**, 126, 10457-10471.

(34) Liu, C.T.; Maxwell, C.I.; Edwards, D.R.; Neverov, A.A.; Mosey, N.J.; Brown, R.S. Mechanistic and computational study of a palladacycle-catalyzed decomposition of a series of neutral phosphorothioate triesters in methanol. *J. Am. Chem. Soc.* **2010**, 132, 16599-16609.

(35) Linstrom, P.J.; Mallard, W.G., NIST Standard Reference Database Number 69; National Institute of Standards and Technology: Gaithersburg, MD, **2005**.

(36) Serpa, F.; Vidal, R.; Filho, J.; Dariva, C.; Franceschi, E.; Santos, A.; Heredia, M.; Banda, G.; Figueiredo, C. Nascimiento, J.; Ciambelli, J. Solubility and Thermodynamic Properties of Carbon Dioxide in MEG/Water Mixtures. *III Iberoamerican Conference on Supercritical Fluids* **2013**, Cartagena de Indias, Colombia, 1-9.

(37) Ambrosetti, A.; Reilly, A.M.; DiStasio Jr., R.A.; Tkatchenko, A. Long-range correlation energy calculated from coupled atomic response functions. *J. Chem. Phys.* **2014**, 140, 18A508.

(38) Peng, H.; Yang, Z.H.; Perdew, J.P.; Sun, J. Versatile van der Waals density functional based on a meta-generalized gradient approximation. *Phys. Rev. X* **2016**, 6, 041005.

(39) Sun, J.; Ruzsinszky, A.; Perdew, J.P. Strongly constrained and appropriately normed semilocal density functional. *Phys. Rev. Lett.* **2015**, 115, 036402.

(40) Schouten, K. J.; Qin, Z.; Pérez Gallent, E.; Koper, M. T. Two pathways for the formation of ethylene in CO reduction on single-crystal copper electrodes. *J. Am. Chem. Soc.* **2012**, 134, 9864-9867.

(41) Montoya, J.H.; Shi, C.; Chan, K.; Nørskov, J.K. Theoretical insights into a CO dimerization mechanism in CO2 electroreduction. *J. Phys. Chem. Lett.* **2015**, 6, 2032-2037.

(42) Luo, W.; Nie, X.; Janik, M.J.; Asthagiri, A., 2015. Facet dependence of CO_2 reduction paths on Cu electrodes. *ACS Catal.* **2015**, 6, 219-229.

(43) Mistry, H.; Choi, Y.W.; Bagger, A.; Scholten, F.; Bonifacio, C.; Sinev, I.; Divins, N.J.; Zegkinoglou, I.; Jeon, H.S.; Kisslinger, K.; Stach, E.A. Enhanced carbon dioxide electroreduction to carbon monoxide over defect rich plasma-activated silver catalysts. *Angew. Chemie Int. Ed.* **2017**, 56, 1-6.

(44) Shustorovich, E.; Bell, A.T. Oxygen-assisted cleavage of O−H, N−H, and C−H bonds on transition metal surfaces: bond-order-conservation-Morse-potential analysis. *Surf. Sci.* **1992**, 268, 397-405.

(45) Bloch, J.; Bottomley, D.J.; Janz, S.; Van Driel, H.M.; Timsit, R.S. Kinetics of oxygen adsorption, absorption, and desorption on the Cu (111) surface. *J. Chem. Phys.* **1993**, 98, 9167-9176.

(46) Soon, A.; Todorova, M.; Delley, B.; Stampfl, C. Oxygen adsorption and stability of surface oxides on Cu (111): A first-principles investigation. *Phys. Rev. B* **2006**, 73, 165424.

(47) López-Moreno, S.; Romero, A.H. Atomic and molecular oxygen adsorbed on (111) transition metal surfaces: Cu and Ni. *J. Chem. Phys.* **2015**, 142, 154702.

(48) Duan, X.; Warschkow, O.; Soon, A.; Delley, B.; Stampfl, C. Density functional study of oxygen on Cu(100) and C(110) surfaces. *Phys. Rev. B* **2010**, 075430.

(49) Baricuatro, J. H.; Ehlers, C. B.; Cummins, K. D.; Soriaga, M. P.; Stickney, J. L.; Kim, Y.-G. Structure and composition of Cu(hkl) surfaces exposed to O_2 and emersed from alkaline solutions: Prelude to UHV-EC studies of CO_2 reduction at well-defined copper catalyst. *J. Electroanal. Chem.* **2014**, 716, 101-105.

(50) Kim, Y.-G.; Soriaga, M. P. Cathodic regeneration of a clean and ordered Cu(100)-(1x1) surface from an air-oxidized and disordered electrode: An operando STM study. *J. Electroanal. Chem.* **2014**, 734, 7-9.

(51) Kim, Y.-G.; Javier, A.; Baricuatro, J. H.; Soriaga, M. P. Regulating the Product Distribution of CO Reduction by the Atomic-Level Structural Modification of the Cu Electrode Surface. *Electrocatalysis* **2016**, 7, 391-399.